Structural transitions with formation of charge-density waves in layer compounds

L. N. Bulaevskiĭ

P. N. Lebedev Physics Institute, USSR Academy of Sciences
Usp. Fiz. Nauk **120**, 259–271 (October 1976)

The current experimental data and theoretical views on structural transitions with formation of charge-density waves (CDW) in layer compounds of transition-metal dichalcogenides are reviewed. The crystallographic data on the parameters of the incommensurate $1T$ and $2H$ modifications are discussed, together with the information on the change in these parameters in transitions to the commensurate state. A microscopic interpretation of the CDW transitions is based on a model of nested regions of the Fermi surface for the $1T$ modification and a saddle-point model for the $2H$ compounds. The fundamental characteristics of transitions from a normal metal to an incommensurate CDW state and from the incommensurate to the commensurate state (change in the period of the superstructure in the layer and perpendicular to the layers) are described on the basis of the phenomenological Ginzburg–Landau theory. Experimental data on changes in the phonon spectrum and the effect of impurities on CDW transitons are also treated.

PACS numbers: 61.50.Qy, 61.70.Rj, 64.80.Gd

CONTENTS

1. INTRODUCTION

Structural phase transitions have been discovered and studied intensively in the last several years in the layer compounds of the transition-element dichalcogenides of the type MX_2, where M = Ta or Nb, and X = Se, Te, or S. A superstructure arises in all these layered metals below a temperature T_0. This involves displacement of atoms from the equilibrium positions of the fundamental structure. As a rule, the period of this superstructure is incommensurate with the period of the fundamental lattice (the lattice above T_0). With further drop in temperature, the superstructure approaches a structure commensurate with the original one, continuously or in jumps. Weighty evidence now favors the idea that the reason for the transitions involves the special geometric properties of the Fermi surface of the conduction electrons of the layered metals. We shall treat below the experimental data on the structural transitions and a microscopic picture that enables one to understand the reason for the transitions and the phenomenological description of the transitions based on the Ginzburg-Landau theory. We shall also discuss the features of the phonon spectrum, both at the transition point T_0 and in the phase having charge-density waves, as well as the effect of impurities on the transitions.

2. GENERAL INFORMATION ON THE STRUCTURE OF THE LAYER COMPOUNDS

The crystals of the layer compounds contain repeating sandwiches consisting of three layers X = M = X. Here the bonding of the metal layer to the chalcogen layers in the sandwich is strong and predominantly covalent, while the bonding between adjacent sandwiches in the crystal is of van der Waals type (Fig. 1). The characteristic distances between the M and X atoms within a sandwich are 1.5–2 Å, while those between adjacent X layers of different sandwiches are about 3 Å. The overlap of the electronic wavefunctions of the metallic layers is small, and the movement of conduction electrons in the layer compounds is near to two-dimen-

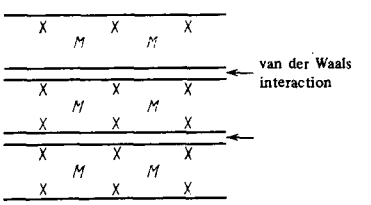

FIG. 1. Arrangement of the layers of atoms of the metal (M) and the chalcogens (X) in the layer compounds.

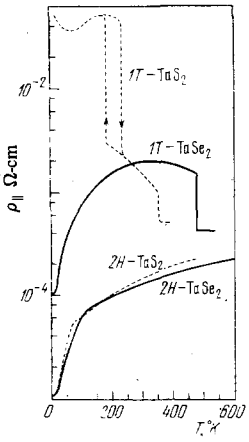

FIG. 2. Temperature-dependence of the resistance along the layers in $1T$-TaS_2, $1T$-$TaSe_2$, $2H$-TaS_2, and $2H$-$TaSe_2$.

sional. This is why the electronic properties of the layered metals is predominantly determined by the structural arrangement of the atoms within the X = M = X sandwich. The structure of the M and X layers is hexagonal. The layers of M and X atoms can be relatively shifted so as to generate a trigonal ($2H$ modification) or octahedral ($1T$ modification) environment of X atoms about M atoms in the sandwich. Compounds of the same composition in different modifications differ very strongly from one another. For example, the $2H$ modifications of $NbSe_2$, $TaSe_2$, and TaS_2 remain metals after the superstructure has set in, and they are superconductors (T_c = 7.4, 0.7, and 0.15 °K, respectively). The $1T$ modifications become semimetals after onset of the superstructure. Trigonal and octahedral sandwiches alternate in the $4Hb$ modification. At low temperatures, the conductivity of $4Hb$-TaS_2 crystals is metallic in terms of its temperature-dependence for movement of electrons along the layers, and semimetallic for movement of carriers in a direction perpendicular to the layers. Detailed information on the structure and electronic properties of the layer compounds has been given in the reviews.[1-4]

3. CHANGE OF ELECTRONIC PROPERTIES IN THE TRANSITIONS

Figure 2 shows the variation in the resistance $\rho_\parallel$ along the layers as a function of the temperature in the crystals $1T$-TaS_2, $1T$-$TaSe_2$, $2H$-TaS_2, and $2H$-$TaSe_2$. In the $2H$ modifications, the structural transition is

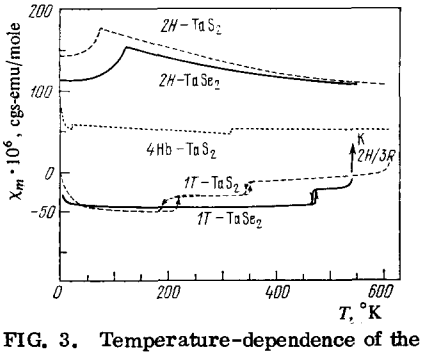

FIG. 3. Temperature-dependence of the magnetic susceptibility in $1T$-$TaSe_2$, $1T$-TaS_2, $2H$-$TaSe_2$, and $2H$-TaS_2.

TABLE I.

Compound		T_0	T_d'	T_d	ΔH cal/mole	$dT_{0,d}/dp$, °K/kbar	References
$2H$	$TaSe_2$	120			1.0		3,5,7,8
				90			
	TaS_2	80					
	$NbSe_2$	35					
$2T$	$TaSe_2$	600					3, 5-7
				473	374	−4.7	
	TaS_2	600					
			352		123	−3.0	
				200	18		
$4Hb$-TaS_2: Octahedral layers				315	110	−5.5	3
Trigonal layers		20					

manifested as a change in slope in the $\rho_\parallel(T)$ relationship (the quantity $\partial\rho_\parallel/\partial T$ increases below T_0) and in a change in sign of the Hall coefficient in the vicinity of T_0. In the $1T$ modifications, the resistance at 500 °K is about an order of magnitude larger than in the $2H$ crystals, and one observes first-order transitions with decreasing temperature in which the resistance increases abruptly (approximately by a factor of two in $1T$-$TaSe_2$ and by an order of magnitude in $1T$-TaS_2). Figure 3 shows the change in magnetic susceptibility in the transitions. We stress that all the transitions below 500 °K in the $1T$ modifications are reversible transitions within a single particular modification. The transitions among the modifications ($1T$, $2H$, $4Hb$, or $6R$) occur above 500 °K, and the enthalpy jump for them is about an order of magnitude larger than for the transitions below 500 °K. They have established in[3,5,6] that the transitions in the $1T$ modifications below 500 °K are transitions from incommensurate to commensurate superstructures, and we shall denote the temperature of these transitions hereinafter as T_d. Apparently the superstructure in the $1T$ crystals sets in at $T_0 \approx 600$ °K (from indirect data).[7] Table I gives the thermodynamic characteristics of the transitions at the points T_0 and T_d for a number of layer compounds (the enthalpy jump ΔH, and the dT_0/dp and dT_d/dp relationships). In $1T$-TaS_2, the transition to the commensurate superstructure occurs in two stages—the first jump is observed at T_d' = 352 °K, and the superstructure below 352 °K is merely close to commensurate though not actually so. At T_d = 200 °K, a transition now occurs to a strictly commensurate structure. In $4Hb$-TaS_2, the changes in structure in the trigonal layers qualitatively resemble the changes in the $2H$ modifications, while those in the octahedral layers resemble those in the $1T$ modifications.

4. STRUCTURAL DATA ON THE TRANSITIONS

The displacements of the atoms upon onset of superstructure are rather small (several percent of the interatomic distance). Hence the onset of superstructure

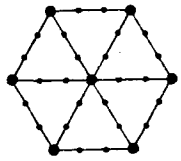

FIG. 4. Reflections from the fundamental structure and from the superstructure[3] in $2H$-$TaSe_2$.

was only discovered five years after the observation of the transitions themselves at the points T_0 and T_d. Most of the data on the superstructures have been obtained by fast-electron diffraction.[3,5,7] The transitions in the $1T$ modifications have also been studied by x-ray structural analysis.[6] The method of elastic and inelastic neutron scattering has recently been used[8] with great success to study the superstructures. The latter method is precisely how the superstructure of the $2H$ modifications has been studied in great detail (it is about an order of magnitude less marked than the superlattice in the $1T$ modifications).

A. The $2H$ modifications

A superstructure sets in at the temperature T_0 in the $2H$ metals in the plane of the layers with an approximately tripled period (Fig. 4). That is, the shifts of the atoms from the equilibrium positions that they had occupied in the high-temperature phase are described by the relationship

$$\mathbf{X}(\mathbf{r}) = \mathbf{X}_1 \sum_{i=1}^{3} \exp[i(\mathbf{Q}_{1i}\mathbf{r} + \Phi_{1i})], \quad \mathbf{Q}_{1i} = \frac{\mathbf{K}_i}{3}(1-\delta), \tag{1}$$

Here $\mathbf{r}$ is the coordinate in the layer, the $\mathbf{Q}_{1i}$ are the three reciprocal wave vectors of the superlattice that make 120° angles with one another and are equal in magnitude, the Φ_{1i} are the phases of the waves, and $\mathbf{K}_i$ are the reciprocal-lattice vectors of the original hexagonal structure of the layer. One finds that $\delta = 0.025$ immediately below T_0 for $TaSe_2$ and $NbSe_2$.[8] According to the experimental data, the density maxima of the superstructure coincide with lines of atoms. Since the maxima of the displacements in (1) are rotated by 30° with respect to the vectors $\mathbf{Q}_{1i}$, the triplet of vectors $\mathbf{Q}_{1i}$ is rotated by 30° with respect to the lines of atoms. Figure 5 shows the directions of the vectors $\mathbf{Q}_{1i}$ in the Brillouin zone of the original two-dimensional hexagonal lattice of the layer, together with the reciprocal-lattice vector $\mathbf{K}_1$ of the layer ($\mathbf{K}_2$ and $\mathbf{K}_3$ are rotated by ± 120° with respect to $\mathbf{K}_1$). The period of the structure in the $2H$ modifications is not altered in the direction perpendicular to the layers. That is, the superstructure is identical in phase in all the layers.

Changes in the superstructure are observed as the temperature falls below the point T_0. The value of δ

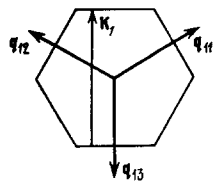

FIG. 5. The Brillouin zone of the layered metals and the orientation of the wave vectors of the superstructure in the $2H$-modifications.

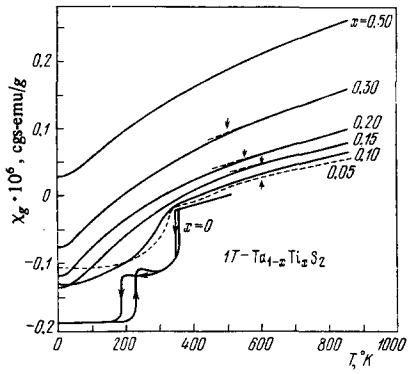

FIG. 6. Temperature-dependence of the magnetic susceptibility[7] in powdered specimens of $1T$-$Ta_{0.96}Tl_{0.04}S_2$, and the method of determining the temperature T_0 of onset of superstructure (arrows) and the temperature T_d of change of superstructure (hysteresis loops).

declines continuously in $NbSe_2$ to reach the value 0.013 at 5 °K. In $2H$-$TaSe_2$, the value of δ falls to 0.005 at 90 °K, and a first-order transition occurs at this point to a commensurate structure having a tripled period within the layer (δ vanishes abruptly).

In addition to the onset of superstructure of (1) in $TaSe_2$ and $NbSe_2$, one finds also displacement waves having the vectors $\mathbf{Q}_{2i} = \mathbf{K}_i - 2\mathbf{Q}_{1i} = \mathbf{K}_i(1+2\delta)/3$ (we shall denote their amplitude and phase by $\mathbf{X}_2$ and Φ_{2i}). The ratio $|\mathbf{X}_2|/|\mathbf{X}_1|$ increases with decreasing temperature (from 0 to 0.3 in $2H$-$TaSe_2$ as the temperature varies from T_0 to $T_d = 90$ °K).

Thus a superstructure arises in the $2H$ metals below T_0 that is incommensurate with the original structure. In $2H$-$NbSe_2$, the incommensurability persists at least to 5 °K according to the data of[8], and even to 1.3 °K from the indirect data of[9]. In $2H$-$TaSe_2$, a transition occurs at the point $T_d = 90$ °K to a commensurate superstructure having a tripled period ($a' = 3a$, $c' = c$).

B. The $1T$ modifications

A superstructure exists in the crystals $1T$-TaS_2 and $1T$-$TaSe_2$ throughout the temperature range in which this modification is stable. That is, the temperature T_0 lies above their transition temperatures to other modifications ($2H$, $4H$, or $3R$). In crystals of $1T$-$Ta_{1-x}Ti_xS_2$ having $x > 0.1$, the $1T$ phase is stable over a broader temperature range. Figure 6 shows the temperature-dependence of the magnetic susceptibility of the alloy with $x = 0.04$, and it also indicates the method of identifying T_d and T_0. These temperatures depend on x (see Chap. 8 below) and extrapolating them to $x = 0$ gives $T_0 \approx 600$ °K in TaS_2 and $TaSe_2$.[7] Below 500 °K, the arrangement of superstructure reflections is analogous to that shown in Fig. 4, but $\mathbf{Q}_{1i} = 0.285\,\mathbf{K}_i$ ($a' = 3.5\,a$). The period of the superstructure in the direction perpendicular to the layers (along the c axis) is tripled, i.e., $c' = 3c$.

At the temperature T_d in $1T$-$TaSe_2$, the vectors $\mathbf{Q}_{1i}$ of the superstructure are rotated by 13°54'. The new lattice has the period $(\sqrt{13})\,a_0$, and it is commensurate

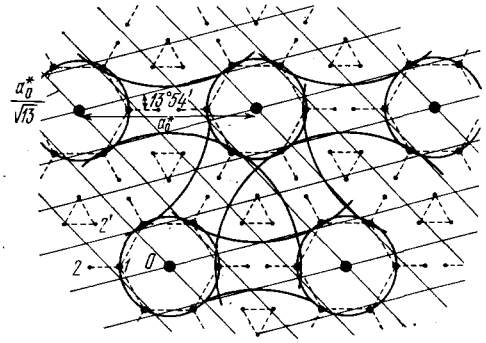

FIG. 7. Fundamental reflections in $1T$-$TaSe_2$ above and below the temperature T_d in the plane of the layers. The dark circles show the reflections above T_d. Below T_d they lie at the nodes of a rhombohedral lattice in the α-orientation.[3]

with the original hexagonal lattice, with 13 atoms lying in the new unit cell. Figure 7 shows the relationship between the reflections above and below T_d, while Fig. 8 shows the arrangement of the points of the new rhombohedral lattice as related to the old hexagonal lattice. We see from Fig. 8 why the 13°54' rotation (= arctan $(\sqrt{3/7})$) makes the superstructure commensurate. We note that $1T$-$TaSe_2$ below T_d shows domains with clockwise and counterclockwise rotation of the superstructure by 13°54' (α- and β domains).

In $1T$-TaS_2, the superstructure from 500° to 352 °K is analogous to the incommensurate superstructure in $1T$-$TaSe_2$. At 352 °K, the superlattice rotates by 12°, while the period along the axis remains tripled. At 200 °K, the superlattice rotates up to 13°54', and it attains the same commensurate superstructure as in $1T$-$TaSe_2$.

The displacements of the lattice atoms in the superstructure give rise to charge-density waves in the crystal (the electronic charge is the same on all atoms in the hexagonal lattice, while the equivalence of the atoms is lost in the superlattice, and the electronic charge on them is redistributed in such a way that the atoms that are closer to one another gain an excess electronic charge). According to the data of the x-ray photoelectron spectra,[10] the charge nonequivalence of the Ta atoms in $1T$-TaS_2 below 200 °K reaches values of the order of one electron per atom. According to the x-ray data of[6], not only the atoms of the metals shift when charge-density waves arise in the $1T$ modifications, but also the chalcogen atoms. Here the displacements of the two types of atoms are opposite in phase. According to the data on quadrupole splitting of the NMR line in $2H$-$NbSe_2$,[11] the non-equivalence of the Nb atoms with respect to electric-field gradient is about 10%. That is, the superstructure of the $2H$ modifications is about an order of magnitude less marked than for the $1T$ modifications (in agreement with the values of their transition temperature T_0). We shall use the abbreviations CCDW and ICDW for the commensurate and the incommensurate CDW, respectively.

5. THE REASONS FOR ONSET OF CDW. THE MODEL OF NESTED REGIONS OF THE FERMI SURFACE

According to the results of Chan and Heine[12] (see also[13]), onset of CDW involves the great increase in the polarizability of the electronic system with decreasing temperature. A structural transition occurs whenever the frequency of any phonon mode becomes very small. Within the framework of the electron-ion Hamiltonian with Coulombic interaction of the electrons and the ions, the frequencies of the longitudinal phonons are determined by the relationship

$$\omega^2(\mathbf{q}) = \omega_0^2[1 - g_0^2(\mathbf{q})\chi(\mathbf{q})], \quad \omega_0^2 = \frac{4\pi NZ^2e^2}{M}, \quad g_0(\mathbf{q}) = i\sqrt{\frac{N}{M\omega_0^2}}\,qV_{ie}(\mathbf{q}), \tag{2}$$

Here N is the density of ions, M is their mass, ω_0 is the plasma frequency of the ions, $g_0(\mathbf{q})$ is the matrix element of interaction of the electrons with the plasma oscillations of the ions, and $\chi(\mathbf{q})$ is the static polarizability of the electronic system. The polarizability of the electronic system with account taken of the Coulombic repulsion of the electrons is expressed in terms of the polarizability $\chi_0(\mathbf{q}, T)$ of noninteracting electrons by using the relationship[10]

$$\chi(\mathbf{q}, T) = \frac{\chi_0(\mathbf{q}, T)}{1 - \left[V(\mathbf{q}) - \frac{1}{2}U\right]\chi_0(\mathbf{q}, T)},$$
$$\chi_0(\mathbf{q}, T) = \sum_{\mathbf{k}} \frac{f(\varepsilon_{\mathbf{k}}) - f(\varepsilon_{\mathbf{q}+\mathbf{k}})}{\varepsilon_{\mathbf{k}} - \varepsilon_{\mathbf{k}+\mathbf{q}}}, \tag{3}$$

Here $V(\mathbf{q})$ is the direct Coulombic interactions of the electrons, U is their exchange interaction, $\varepsilon_{\mathbf{k}}$ is the energy of the electrons, and $f(\varepsilon)$ is the Fermi distribution function. The system becomes unstable if the polarizability $\chi_0(\mathbf{q}, T)$ becomes large in it, and the following condition is satisfied:

$$g_0^2(\mathbf{q}) + \frac{U}{2} - V(\mathbf{q}) = \frac{1}{|\chi_0(\mathbf{q}, T)|}. \tag{4}$$

Equation (4) determines the transition temperature and the wave vectors $\mathbf{Q}_i$ of the superstructure. In order for CDW to arise, the electron-phonon interaction must be larger than the Coulombic interaction. That is, the condition $g_0^2(\mathbf{q}) > V(\mathbf{q})$ must be satisfied. Otherwise (when $g^2(\mathbf{q}) < V(\mathbf{q})$), the system proves to be un-

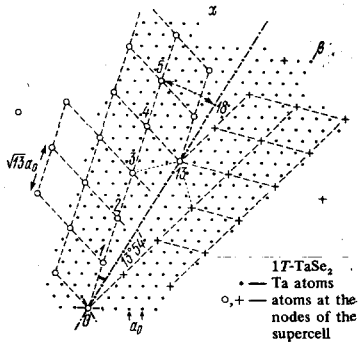

FIG. 8. Superlattice in $1T$-$TaSe_2$ below T_d. The α- and β-domains and the unit cell of the commensurate phase having the period $(\sqrt{13})\,a_0$ are shown.

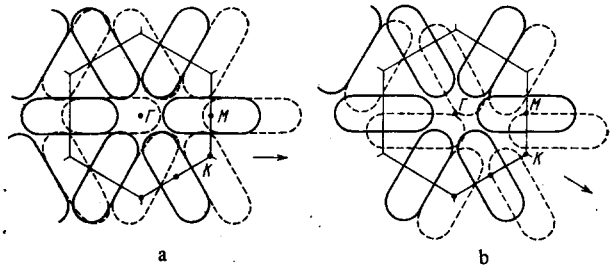

FIG. 9. The Fermi surface for wave vectors lying within the layer, and the extent of nesting of the flat regions upon shifting by a vector lying parallel to the line ΓM(a), or by a vector parallel to the line ΓK(b).[3]

stable with respect to formation of spin-density waves (this transition is realized in chromium).[12] Overhauser[14] thought that onset of spin-density waves (SDW) is favorable when the Coulombic interaction is very large while $\chi_0(\mathbf{q}, T)$ has an ordinary value. However, the approximation that he used seems to be unsuitable in this case, and Wigner crystallization of the electron gas proves to be more favorable in the situation that he treated. In systems for which Eqs. (2) and (3) are applicable, the electron-phonon and Coulombic interactions cannot be very large, and the condition (4) is reached when the electronic polarizability $\chi_0(\mathbf{q}, T)$ becomes large. For an isotropic Fermi surface, $\chi_0(\mathbf{q}, T)$ has a Kohn anomaly at $q = 2k_F$. However, here the derivative $\partial\chi_0(q, T)/\partial q$ is large when $q = 2k_F$, but not the quantity $\chi_0(q, T)$ itself. Yet if the Fermi surface has regions that nest together upon shifting by the wave vector $\mathbf{Q}_i$, then $\chi(\mathbf{Q}_i) \sim N(0)\ln(\varepsilon_F/T)$ as $T \to 0$.[15,16] Here $N(0)$ is the density of states at the Fermi surface, and ε_F is the Fermi energy.

The conditions for onset of CDW are favorable in the layer compounds, owing to the rather strong electron-phonon interaction, the almost two-dimensional nature of the Fermi surface, and the existence of flat regions on the two-dimensional Fermi surface. Mattheiss[17] has calculated the band structure of the 1*T* and 2*H* modifications, and Fig. 9 shows the two-dimensional Fermi surface for 1*T*-$TaSe_2$. This diagram shows the flat regions and their degree of nesting upon displacement along the lines ΓM and ΓK. The ΓM shift proves to be more favorable, since here the flat regions on four segments of the Fermi surface nest together, rather than on two (as in the shift along ΓK), though the length of the nested regions per segment proves to be less. According to the experimental data, the vector $\mathbf{Q}_{11}$ actually lies along ΓM. According to Mattheiss' calculations, the Fermi surface intersects the line MK

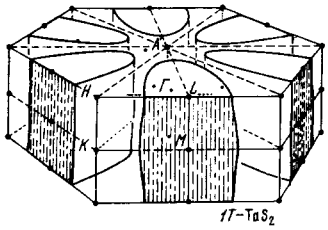

FIG. 10. The Fermi surface in 1*T*-TaS_2 according to Mattheiss' calculations.[3,17]

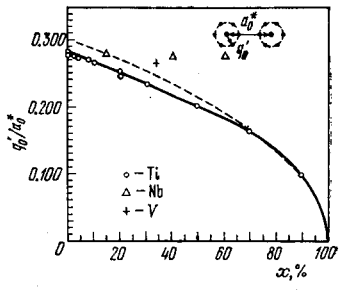

FIG. 11. Relationship of the magnitude of the superstructure wave vector[3] Q_{1i} to the fraction x of metal atoms in the compounds 1*T*-$Ta_{1-x}M_xS_2$ with M = Ti, Nb, or V.

to cut off a segment of 0.59 MK from it as we move from M to K. According to the experimental data, the magnitude of Q_{11} gives the value 0.43 for this. We can deem the agreement to be quite satisfactory in view of the simplifications that Mattheiss has made. The agreement of the experimentally determined and theoretically calculated values of Q_{11} proved to be even better in calculations by the Korringa-Kohn-Rostoker method. The corresponding calculations[18] give the value 0.34 for Q_{11}/K_1 below T_0 for 1*T*-TaS_2, and 0.32 for 1*T*-$TaSe_2$. The experimental data for these same quantities[3] are 0.288 ± 0.005 and 0.285 ± 0.006, respectively.

We note that Mattheiss' calculations have confirmed the two-dimensional nature of the band structure of the layer compounds. Figure 10 shows the complete three-dimensional Fermi surface for 1*T*-TaS_2. We see that the electron energy varies very slightly as the wave vector passes along the line *LM*, which is perpendicular to the plane of the layers.

In order to confirm the hypothesis of onset of CDW owing to the presence of nesting regions on the Fermi surface, the values of the wave vectors $\mathbf{Q}_{1i}$ of the superstructure of the alloys 1*T*-$Ta_{1-x}M_xS_2$ (M = Ti, Nd, V) were measured. Replacement of Ta by Ti decreases the number of electrons in the conduction band (Ta, Nb, and V atoms contribute one electron to the conduction band, while a Ti atom contributes none). A parabolic relationship of $\mathbf{Q}_{1i}$ to x was obtained above T_d in the compound with M = Ti (Fig. 11), and Q_{11} is practically independent of x for M = Nb or V. Comparison of the data for M = Ti and M = Nb or V implies that the decrease of $\mathbf{Q}_{11}$ in the alloy with M = Ti mainly involves the decreased concentration of conduction electrons. According to Mattheiss' calculations, the $\varepsilon(\mathbf{k})$ relationship is parabolic as $\mathbf{k}$ varies along the line ΓM (the relationship changes as we approach the point Γ—the curve becomes flatter). In this case the dependence of Q_{11} on the concentration of electrons, i.e., on $(1-x)$ should actually be parabolic, as is observed experimentally. The agreement of the theoretical calculations of the quantity $Q_{11}(x)$[18] with the experimental relationship is also quite good.

The onset of the superstructure below T_0 is accompanied by onset of an energy gap in the nesting regions of the Fermi surface. Hence the model of nesting regions of the Fermi surface explains the decrease in conductivity and magnetic susceptibility at the point T_0 of crystals of the 1*T* modification (see Fig. 6). According to optical studies[19] in 1*T*-TaS_2 below 380 °K, the

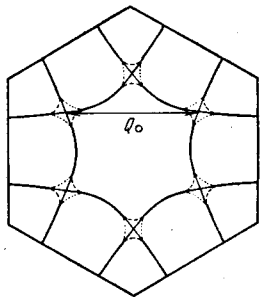

FIG. 12. The two-dimensional Fermi surface for $2H$-$NbSe_2$ according to the calculations of Mattheiss (schematic).

absorption spectrum at energies below 0.5 eV shows a weak structure that is not characteristic of a metallic system of electrons. The absorption in the 0.04–0.5 eV region declines with decreasing temperature, but no clear signs of a gap arise.

Thus, the model of nesting regions of the Fermi surface describes the situation well in the $1T$ modifications. This model enables one to explain the magnitude and direction of the vectors $\mathbf{Q}_{1i}$, and it qualitatively explains the change in the electronic properties during the transitions. Yet is hard to understand the properties of the $2H$ crystals on the basis of this model. According to the data of[19], a structure appears in the absorption spectrum of $2H$-$TaSe_2$ below 80 °K that is characteristic of a gap of 0.25 eV. This value seems too large for a transition temperature of 80 °K—such a large ratio Δ/T_0 can hardly be obtained in the nesting-region model. The increase in $\partial\rho_\parallel/\partial T$ below T_0 and the nature of the change in the magnetic susceptibility in the transition also do not agree with the predictions of this model.

Rice and Scott[20] have proposed another model that explains the onset of CDW in the $2H$ crystals. Figure 12 shows the Fermi surface of $2H$-$NbSe_2$ as obtained by Mattheiss. The central part of the Brillouin zone corresponds to hole conduction, and the peripheral parts to electronic conduction. These regions make contact at saddle points, and if the Fermi surface passes near the saddle points, then the electronic polarizability $\chi(\mathbf{Q})$ increases logarithmically with decreasing temperature when $\mathbf{Q}$ is the vector joining the saddle points (if $kT \gg \varepsilon_F'$, where ε_F is measured from the saddle point). This model can qualitatively explain the large value of Δ/T_0, the small change in the density of states during the transition, the sign of the variation $\partial\rho_\parallel/\partial T$, the peak in the magnetic susceptibility near the transition point, and the change in the sign of the Hall coefficient in the transition. However, the theory of Rice and Scott is based on the very strong assumption that the Fermi level is close to the saddle points. Therefore we cannot consider the problem of its applicability to the $2H$ crystals as being fully solved. Within the framework of this model, a change in the concentration of electrons (replacement of Ta by Ti in the $2H$-$Ta_{1-x}Ti_xSe_2$ alloys) should greatly diminish T_0. Such experiments have not yet been performed.

Thus the microscopic models of the transitions fundamentally predict only qualitatively the change in the lattice and the electronic properties at the point T_0. Quantitative calculations of the change in the electronic spectrum in a CDW transition have not yet been made. The microscopic models are not yet in a condition to give any information on ICDW–CCDW transitions. Yet one can draw many qualitative and quantitative conclusions on the normal metal–ICDW and ICDW–CCDW transitions based on the Ginzburg-Landau macroscopic theory of phase transitions. In particular, this theory describes very well the transitions between the superstructures of the $1T$ and $2H$ modifications and the temperature-dependence of the vectors $\mathbf{Q}_{1i}$ in $2H$-$NbSe_2$ and $2H$-$TaSe_2$.

6. THE PHENOMENOLOGICAL THEORY OF CDW TRANSITIONS

We can take as the order parameter of a CDW transition the displacement of the atoms from the equilibrium positions $\mathbf{X}(\mathbf{r})$ or the change in electron density—these two quantities depend linearly on one another. The description in terms of electron density is simpler, but it gives no information on the magnitude and direction of the displacements of the atoms in the superstructure. The currently existing phenomenological theory[8,21,22] uses as the parameter the relative change $\alpha_n(\mathbf{r})$ in the electron density in the layer. Its expansion in terms of plane waves having the wave vectors $\mathbf{Q}_{1i}$ in the layer and the wavenumbers p_i along the c axis has the form

$$\alpha_n(\mathbf{r}) = \mathrm{Re}\sum_i \psi_{in}(\mathbf{r}),\quad \psi_{in}(\mathbf{r}) = u_i \exp(i\mathbf{Q}_{1i}\mathbf{r} + ip_i n + \Phi_i), \tag{5}$$

Here u_i is the amplitude of the waves $(\mathbf{Q}_{1i}, p_i)$ and Φ_i is their phase. The Ginzburg-Landau free energy for the parameter $\alpha_n(\mathbf{r})$ has the form

$$\begin{aligned} F = \sum_n \int d\mathbf{r} \Big\{ & a(\mathbf{r})\alpha_n^2 - b(\mathbf{r})\alpha_n^3 + c(\mathbf{r})\alpha_n^4 + d(\mathbf{r})[|\psi_{1n}\psi_{2n}|^2 \\ & + |\psi_{2n}\psi_{3n}|^2 + |\psi_{1n}\psi_{3n}|^2] + \sum_i [e(\mathbf{r})|(\mathbf{Q}_i\nabla - iQ_i^2)\psi_{in}|^2 \\ & + f(\mathbf{r})[\mathbf{Q}_i\nabla\psi_{in}]^2] + \sum_{n'} \int d\mathbf{r}' g_{nn'}(\mathbf{r}, \mathbf{r}')\alpha_n(\mathbf{r})\alpha_{n'}(\mathbf{r}') \Big\}, \end{aligned} \tag{6}$$

where the coefficients a, b, c, d, e, f, and g depend periodically on the coordinates with the period of the original lattice, i.e., for example,

$$c(\mathbf{r}) = c_0 + c_1 \sum_i \cos \mathbf{K}_i\mathbf{r}. \tag{7}$$

The last term in (7) describes the Coulombic interaction of the CDW's of different layers. This interaction declines exponentially with increasing distance between layers, and we can restrict the treatment in practice to accounting for the interaction of adjacent layers alone. As usual, $a_0 = a'(T - T^*)$, and the terms containing the gradients determine the magnitude and direction of the CDW wave vectors. The free energy of (6) with account taken of the dependence of the coefficients on $\mathbf{r}$ describes the following effects that have been detected experimentally:

a) The first-order transition at the point T_0 ($\neq T^*$) from the normal state to the CDW state having three waves arises from the cubic term in α.[21] It is evident

from the microscopic picture of the causes of the transition that the vectors $\mathbf{Q}_i$ are generally incommensurate with the vectors $\mathbf{K}_i$, and the superlattice will be incommensurate below T_0, since the vectors $\mathbf{Q}_{1i}$ must be equal to $\mathbf{Q}_i$ near T_0. Owing to the same cubic term, the period of the incommensurate superstructure along the c axis can be either tripled or the same as in the original lattice. In the $1T$ modifications, the adjacent layers of the original lattice are equivalent, the Coulombic interaction is minimal when $c' = c$, and a tripled period of the superlattice arises. In the $2H$ modifications, the adjacent layers of the original lattice are nonequivalent, and the case $c' = c$ is found experimentally.

b) In the case of incommensurate CDW, the appearance of the wave $\mathbf{Q}_{1i}$ arising from the terms having the coefficients b_1, c_1, etc., unavoidably entails the appearance of harmonics of the superstructure of the type $\mathbf{Q}' = n\mathbf{Q}_{1i} + m\mathbf{K}_i$, where n and m are integers. Owing to the gradient terms, the only large amplitudes are those of the harmonics for which $|\mathbf{Q}'| \approx |\mathbf{Q}_i|$. This situation is realized in the $2H$ modifications, since $|\mathbf{Q}_i| \approx |\mathbf{K}_i/3|$ for them, and the harmonics having $\mathbf{Q}_{2i} = \mathbf{K}_i - 2\mathbf{Q}_{1i}$ also have a value of $|\mathbf{Q}_{2i}|$ close to $|\mathbf{K}_i/3|$, and thus to $|\mathbf{Q}_i|$. Therefore the amplitude of the harmonics $\mathbf{Q}_{2i}$ in $2H$-$TaSe_2$ is rather large, and as we go away from the point T_0, it approaches the amplitude of the fundamental superstructure. The presence of the harmonics $\mathbf{Q}_{2i}$ causes the actual wave vectors $\mathbf{Q}_{1i}$ of the superstructure to depart from $\mathbf{Q}_i$ as we go away from the point T_0. In $2H$-$NbSe_2$ and $2H$-$TaSe_2$, the vectors $\mathbf{Q}_{1i}$ and $\mathbf{Q}_{2i}$ approach $\mathbf{K}_i/3$ with decreasing temperature. In $2H$-$TaSe_2$ at the temperature T_d, this change ends in a first-order transition to a commensurate superstructure having $Q_{1i} = K_i/3$. A description of all these effects within the framework of the free energy of (6) and the corresponding measurements of the superstructure are given in[8].

c) In the $1T$ modifications, the transition to a commensurate superstructure does not arise from the cubic, but the fourth-order terms in α having the coefficients c_1. A rotation of the vectors $\mathbf{Q}_i$ by 13°54' from the direction ΓM has the result that the new vectors $\mathbf{Q}_i$ satisfy the relationships

$$\begin{aligned} 3\mathbf{Q}_i - \mathbf{Q}_{i+1} &= \mathbf{K}_i, \qquad i = 1, 2, 3, \quad \mathbf{Q}_4 \equiv \mathbf{Q}_1; \\ 3p_i - p_{i+1} &= 2\pi m_i, \quad p_4 \equiv p_1. \end{aligned} \tag{8}$$

The relationships (8) give $(\sqrt{13})a$ as the period of the new unit cell, and they give a 13-fold period along the c axis in the commensurate structure.[21,22]

7. CHANGES IN THE PHONON SYSTEM IN CDW TRANSITIONS

As the point T_0 is approached, the phonons must become softened that have the wave vectors $\mathbf{Q}_i$ and show polarization in the direction of the static displacements of the ions in the superstructure. A softening of phonons having the momenta $\mathbf{Q}_i$ and a polarization along the layer has been observed by inelastic neutron scattering in[8] for $2H$-$TaSe_2$. However, even at 130 °K ($T_0 = 120$ °K), the gap in the frequencies of phonons having the momenta $\mathbf{Q}_i$ reached only 0.0015 eV for an initial phonon frequency of 0.007 eV. The reason for the incomplete softening of phonons in $2H$-$TaSe_2$ remains as yet unclear. It is not ruled out that the mode that is almost completely softened in the transition is a superposition of displacements of atoms along the layers and displacements in the direction perpendicular to the layers (in this regard, see[23]).

The specifics of the phonon spectrum of the CDW state has not yet been studied experimentally. According to the theoretical ideas,[21,24] the phonon branches at lowest frequencies in the CDW state involve oscillations of the phases of the superstructure. These oscillations correspond to modulation of the period of the wave, and they therefore involve local variations in the electron density. In the ICDW state, the free energy of (6) fixes only the sum of the phases Φ_i. Therefore, if we don't account for the Coulomb interaction of the electrons in the layer, the frequency of the two phonon modes must vanish in the limit of long-wavelength vibrations (one of these modes is longitudinal, and the other transverse). The Coulomb interaction causes the frequency of the longitudinal mode $\omega_L(\mathbf{q})$ to differ from zero as $\mathbf{q} \to 0$, and one transverse mode of phase oscillations of the superstructure must exist in the ICDW state along with the sonic spectrum. The problem of the interactions of this mode with the corresponding sonic mode of the fundamental lattice has not yet been studied.

8. THE EFFECT OF IMPURITIES ON CDW TRANSITIONS

Impurities smear out the nesting (in momentum space) regions of the Fermi surface. Hence, introduction of impurities or defects into crystals of the layer compounds should lower the transition temperature T_0 or completely suppress the CDW transitions. The results of theoretical calculations of the effect of disorder on the temperature T_0 of CDW transition in quasi-one-dimensional structures (Peierls transition) have been presented in[25] and in the review[26]. The corresponding calculations for the layer compounds have not yet been made. It is evident from general considerations that the effect of disorder on ICDW–CCDW transitions must be even stronger, but a microscopic theory of such transitions that would enable one to calculate T_d has not yet been devised. In[21], the phenomenological Ginzburg-Landau theory was used to describe the effect of impurities, and the following term was added to Eq. (6):

$$\int d\mathbf{r} \rho_0(\mathbf{r})\, \alpha(\mathbf{r})\, U(\mathbf{r}). \tag{9}$$

Here $\rho_0(\mathbf{r})$ is the charge density of the original lattice, and $U(r)$ is the chaotic potential of the impurities. A theory of this type accounts for the effect of impurities on the ordering of the CDW phase, yet it fully ignores the effect of the impurities on the movement of electrons and the temperature-dependence of the polariz-

ability of the electronic system. No theory yet exists that accounts for both aspects of the effect of disorder on CDW transitions.

The effect of impurities on the points T_0 and T_d has been studied experimentally for the $1T$ modifications.[7] In the system $1T$-$Ta_{1-x}Ti_xS_2$, they got $dT_0/dx = -3\,^\circ K$/at. %, and in $1T$-$Ta_{1-x}Nb_xS_2$ they found $dT_d'/dx = -12\,^\circ K$/at. %, while the transition at the point T_d disappears when $x > 0.005$. The concentration of electrons does not vary with increasing x in this alloy. Therefore all the changes in T_d and T_d' involve lattice disorder. The anion disorder in the compound $1T$-$TaS_{2-x}Se_x$ gives rise to a monotonic variation in T_d: with increasing x, T_d varies from 473 °K (T_d for $1T$-$TaSe_2$) to 350 °K ($1T$-TaS_2), and the curve of the $T_d(x)$ relationship passes everywhere below the straight line passing between the points 473 and 350 °K.

Intercalation of the layer compounds of the $2H$ modifications also lowers the temperature T_0 or completely suppresses the CDW transition. This apparently involves the fact that the intercalated molecules have dimensions incommensurate with the period of the unit cell of the layers. Thus intercalation changes the structure of the layers and gives rise to lattice defects.

We note in conclusion that CDW transitions undoubtedly affect the critical temperature of the superconducting transition of the $2H$ metals—suppression of the transitions increases T_c (see the reviews[2,4]). The effect of the transitions on the magnetic properties of layered superconductors has been discussed in[4], and more detailed results are contained in[27].

[1]J. A. Wilson and A. D. Yoffe, Adv. Phys. 18, 193 (1969).
[2]A. D. Yoffe, Festkörperprobleme 13, 1 (1973); Ann. Rev. Mater. Sci. 3, 147(1973).
[3]J. A. Wilson, F. J. Di Salvo, and S. Mahajan, Adv. Phys. 24, 117 (1975).
[4]L. N. Bulaevskiĭ, Usp. Fiz. Nauk 116, 449 (1975) [Sov. Phys. Usp. 18, 514 (1975)].
[5]J. A. Wilson, F. J. Di Salvo, and S. Mahajan, Phys. Rev. Lett. 32, 882 (1974).
[6]P. M. Williams, G. S. Parry, and C. B. Scruby, Phil. Mag. 29, 695(1973); C. Scruby, P. M. Williams, and G. S. Parry, *ibid.* 31, 225 (1975).
[7]F. J. Di Salvo, J. A. Wilson, B. G. Bagley, and J. V. Wasczak, Phys. Rev. B12, 2220 (1975).
[8]D. E. Moncton, J. D. Axe, and F. J. Di Salvo, Phys. Rev. Lett. 34, 734 (1975).
[9]M. Barmatz, L. R. Testardi, and F. J. Di Salvo, Phys. Rev. B12, 4367 (1975).
[10]G. K. Wertheim, F. J. Di Salvo, and S. Chiang, Phys. Lett. A54, 304 (1975).
[11]E. Ehrenfreund, A. C. Gossard, F. R. Gamble, and T. H Geballe, J. Appl. Phys. 42, 1491 (1971).
[12]S.-K. Chan and V. Heine, J. Phys. F3, 795 (1973).
[13]E. G. Maksimov, Zh. Eksp. Teor. Fiz. 69, 2236 (1975) [Sov. Phys. JETP 42, 1138 (1975)].
[14]A. W. Overhauser, Phys. Rev. 128, 1437 (1962); 167, 691 (1968); J. Rath and J. Callaway, Phys. Rev. B8, 5398 (1971).
[15]W. M. Lomer, Proc. Phys. Soc. 80, 489 (1962).
[16]A. M. Afanas'ev and Yu. M. Kagan, Zh. Eksp. Teor. Fiz. 43, 1456 (1962) [Sov. Phys. JETP 16, 1030 (1963)].
[17]L. F. Mattheiss, Phys. Rev. B8, 3719 (1973).
[18]H. W. Myron and A. J. Freeman, *ibid.* B11, 2735 (1975).
[19]A. S. Barker, J. A. Ditzenberger, and F. J. Di Salvo, *ibid.* B12, 2049.
[20]T. M. Rice and G. K. Scott, Phys. Rev. Lett. 35, 120 (1975).
[21]W. L. McMillan, Phys. Rev. B12, 1187 (1975).
[22]L. N. Bulaevskiĭ and D. I. Khomskiĭ, Pis'ma Zh. Eksp. Teor. Fiz. 23, 584 (1976) [JETP Lett. 23, 532 (1976)].
[23]M. J. Rice, C. B. Duke, and N. O. Lipari, Sol. State Comm. 17, 1089 (1975).
[24]T. M. Rice, *ibid.* 17, 1055 (1975).
[25]L. N. Bulaevskiĭ and M. V. Sadovskiĭ, Fiz. Tverd. Tela (Leningrad) 16, 1159 (1974) [Sov. Phys. Solid State 16, 743 (1974)].
[26]L. N. Bulaevskiĭ, Usp. Fiz. Nauk 115, 263 (1975) [Sov. Phys. Usp. 18, 131 (1975)].
[27]L. N. Bulaevskiĭ, A. A. Guseĭnov, and A. I. Rusinov, Zh. Eksp. Teor. Fiz. 72, No. 1 (1976) [Sov. Phys. JETP 45, No. 1 (1976)].

Translated by M. V. King